TISSUE ENGINEERING: Part C
Volume 20, Number 2, 2013

DOI: 10.1089/ten.tec.2012.0771

Methods Article

In Vitro Method for Real-Time, Direct Observation of Cell–Vascular Graft Interactions Under Simulated Blood Flow

Joseph S. Uzarski, PhD, Aurore B. Van de Walle, MS, and Peter S. McFetridge, PhD

In the development of engineered vascular grafts, assessing the material's interactive properties with peripheral blood cells and its capacity to endothelialize are important for predicting *in vivo* graft behavior. Current *in vitro* techniques used for characterizing cell adhesion at the surface of engineered scaffolds under flow only facilitate a terminal quantification of cell/surface interactions. Here, we present the design of an innovative flow chamber for real-time analysis of blood–biomaterial interactions under controllable hemodynamic conditions. Decellularized human umbilical veins (dHUV) were used as model vascular allografts to characterize platelet, leukocyte, and endothelial cell (EC) adhesion dynamics. Confluent EC monolayers adhered to the lumenal surface of the grafting material were flow conditioned to resist arterial shear stress levels (up to 24 dynes/cm^2) over a 48 h period, and shown to maintain viability over the 1 week assessment period. The basement membrane was imaged while whole blood/neutrophil suspensions were perfused across the HUV surface to quantify cell accumulation. This novel method facilitates live visualization of dynamic events, including cell adhesion, migration, and morphological adaptation at the blood–graft interface on opaque materials, and it can be used for preliminary assessment of clinically relevant biomaterials before implantation.

Introduction

Cell adhesion is a critical consideration for implantable biomedical devices, particularly in vascular grafts where appropriate surface properties are critical to graft success. Thrombus formation, characterized by excessive platelet adhesion and aggregation, is a significant cause of occlusive failure of vascular grafts.[1,2] As such, persistent efforts have been made to produce materials that are resistant to protein adsorption and peripheral cell attachment.[3] As part of the design process, an important precursor to clinical implantation is a global assessment of the biomaterial's inherent reactivity with blood.[4] Preclinical characterization of a material's resistance to cellular adhesion and infiltration has typically been assessed *in vivo* using vascular bypass[5] or *ex vivo* shunt models.[6] While bypass surgeries are useful for predicting long-term patency of implanted biomaterials, a significant drawback is that assessment can only be performed terminally. *Ex vivo* shunt models were developed to allow real-time assessment of blood cell accumulation using radiolabeled platelets.[7] Animal trials are expensive and time consuming, however, and more conservative strategies that offer a higher throughput while being cost effective have been sought.

Adhesion of circulating blood cells is a dynamic process that is mediated by the mechanical forces associated with blood flow. Due to the difficulties associated with (1) accurately measuring variable hemodynamic forces across different vascular geometries and (2) imaging peripheral cell adhesion events *in vivo*, parallel plate flow chambers have been used to simulate these processes in a more controllable *in vitro* setting. These devices produce a parabolic flow velocity profile between two planar surfaces, subjecting each surface to uniform fluid shear stress (SS).[8–10] Glass, polystyrene, or other optically transparent substrates can then be coated with cells or proteins, or micropatterned with selectively adhesive peptides/non-adhesive monomers to observe cell adhesion under flow using conventional light microscopy. Much of our current understanding of the role shear plays in cell signaling, protein conformational changes, and other phenomena associated with peripheral cell adhesion has been obtained through the use of parallel plate chambers.[8,11]

Given the practical advantages of real-time, non-invasive imaging of circulating cell adhesion without the need for expensive imaging systems, we sought to develop a device that could be used to monitor these events on the surfaces of clinically implantable vascular biomaterials. Here, we detail the design of a novel parallel plate flow chamber for real-time observation of peripheral cell adhesion and morphological adaptation on opaque vascular biomaterials under controlled shear stresses. Using labeled whole blood and

J. Crayton Pruitt Family Department of Biomedical Engineering, University of Florida, Gainesville, Florida.

select cell suspensions, we demonstrate the capability of this device to permit live capture of dynamic cell adhesion events at the intimal surface of naturally derived blood vessels using time lapse fluorescence microscopy. We also validate the use of this flow chamber for long-term culture of neo-endothelia and optimize a flow preconditioning regime that yields confluent endothelial cell (EC) monolayers which are resistant to arterial shear stresses. These assays demonstrate the versatility of this device for improved *in vitro* modeling of physiological cell adhesion events as they occur *in vivo*.

Materials and Methods

Cell culture

Human umbilical vein endothelial cells (HUVEC) were sourced from umbilical cords obtained from the Labor and Delivery unit at Shands Hospital at the University of Florida and processed within 12 h of birth. EC were isolated from cords using collagenase perfusion, as previously described by Jaffe *et al*.[12] Cells were maintained in VascuLife basal medium supplemented with VEGF LifeFactors kit (LifeLine Cell Technologies) and 100 U/mL penicillin/streptomycin (HyClone) at 37°C with 5% CO_2, and used experimentally between P2 and P5.

HL-60 promyelocytic leukemia cells transduced with a green fluorescent protein (GFP)-expressing lentiviral vector were generously provided by Dr. Christopher Cogle (University of Florida Department of Medicine). They were maintained at 5×10^5–2×10^6 cells/mL in Dulbecco's modified Eagle Medium (Hyclone) supplemented with 20% fetal bovine serum (FBS).

Blood draws

Human venous blood was harvested from healthy adult volunteers after obtaining informed consent (IRB approval #689-2010). Blood was collected in 10 U of heparin using a 21-gauge needle. Platelets were fluorescently labeled with 20 μg/mL of Acridine Orange (Molecular Probes) and used immediately in perfusion experiments.

Dissection and decellularization of human umbilical veins

Human umbilical veins (HUV) were isolated from the surrounding tissue using an automated dissection procedure that has been previously described.[13] In brief, umbilical cords were rinsed clean and cut into 10 cm sections. A stainless steel mandrel (1/4″ outside diameter (OD)) was inserted through the vein and then progressively frozen down to −80°C. After at least 24 h, frozen cords were machined to a uniform wall thickness of 750 μm using a CNC lathe (MicroKinetics). Veins were progressively thawed at −20°C for 2 h and then at 4°C for 2 h. Veins were decellularized by immersion in 1% (w/v) solution of sodium dodecyl sulfate (SDS) in DI water under orbital shaking (100 rpm) for 24 h at a 1:20 mass to volume ratio. Decellularized HUV (dHUV) were sequentially rinsed in DI water solutions under orbital shaking for 5 min, 15 min, 40 min, 1 h, 3 h, 12 h, and 24 h. dHUV sections were then incubated in 70 U/mL of deoxyribonuclease I (Sigma-Aldrich) in phosphate-buffered saline (PBS) agitated on an orbital shaker for 2 h at 37°C. Sections were rinsed in DI water (2×) for 5 min and terminally sterilized in a solution of 0.2% peracetic acid and 4% ethanol in DI water on an orbital shaker for 2 h. Scaffolds were sequentially rinsed for 5 min, 15 min, 40 min, and 1 h in DI water, and pH balanced in PBS (pH 7.40) for 24 h. Scaffolds were stored in PBS at 4°C for a maximum of 2 weeks until use.

Estimation of flow velocities

GFP+ HL-60 cells were passed through the flow chamber at a constant flow rate while time lapse imaging was conducted. The objective (5×) was focused at a position halfway between the imaging window and the lumenal HUV surface in the *z*-direction. HL-60 cells passing through the flow field were imaged at various increments from the center of the channel to the side wall. Velocity was calculated using AxioVision software by measuring the distance traveled by the same cell in two consecutive frames and dividing it by the time elapsed. $N=10$–20 cells were measured at each zone presented.

Platelet adhesion (acellular scaffolds)

With the HUV mounted into the flow chamber, whole blood was perfused across the HUV surface at a wall SS of 2 dynes/cm^2, which was calculated according to the Hagen–Poiseuille equation:

$$\tau = \frac{6\mu Q}{bh^2} \quad (1)$$

where μ is viscosity, Q is mean volumetric flow rate, and b and h are the base width and channel height, respectively. A longpass emission filter (>530 nm) was used to detect fluorescently labeled platelets using RNA binding acridine orange (Molecular Probes; 460/650 nm). Platelets were perfused continuously over a 5 min period, and images were captured every 15 s for a dynamic observation of aggregate formation. At 1 min intervals, a threshold was applied to obtain a representative black and white mask of each image with the percentage of white area corresponding to the percentage of platelet coverage. Platelet aggregate growth was quantified by measuring length in the flow direction at 1 and 5 min ($n=6$ aggregates).

The light intensity profiles of platelet aggregates were measured using NIH ImageJ software. Gray value (with white corresponding to the highest light intensity, and black corresponding to the lowest) was determined along a line parallel to the flow direction and traversing the middle of the aggregate with regard to its width. Light intensity profiles of seven aggregates were plotted and thresholded at 10% of the gray value range to distinguish each aggregate from the HUV background. Skewness of each thresholded aggregate was determined as a measure of symmetry; results are presented as mean ± standard error. Aggregate length was normalized by rescaling each aggregate out of 100 pixels, and gray value data were discretized by averaging all points within a five-pixel length range. The plot obtained gave a global platelet aggregate light intensity profile.

Perfusion culture system

Assembled flow chambers were connected to a media reservoir fitted with a 0.22 μm filter for gas exchange. The entire

system was placed in a dry incubator maintained at 37°C and 5% CO_2. The flow rate through the chamber was directly modulated by the rotational speed of the peristaltic pump, which was controlled by Masterflex Linkable Instrument Control Software V3.1. The mean wall SS to which EC were exposed was calculated according to Equation (1) (assuming steady flow) as described earlier. SS amplitude was similarly calculated from the flow rates measured at the maximum/minimum pressures observed during a single pulsation. The Reynolds number (Re) was calculated according to

$$Re = \frac{\rho Q}{b\mu} \tag{2}$$

where Q is volumetric flow rate, ρ is the density of water at 37°C, b is the base width of the flow field, and μ is the viscosity of water at 37°C. At the maximum flow rate, the Reynolds number was calculated to be 332, indicating laminar flow. The entrance length (Le) for fully developed flow, which was calculated according to

$$\frac{Le}{h} = 0.06Re \tag{3}$$

where Re is the Reynolds number and h is the height of the flow field, was determined to be 11.96 mm. Since the viewing window was located 15 mm from the flow field entrance, the area under analysis was subjected to a fully developed laminar flow.

EC seeding

Assembled flow circuits were sterilized with a solution of 4% ethanol, 0.2% peracetic acid for 2 h and balanced with PBS (pH 7.4). Standard EC media (2% FBS) were allowed to flow through the system before seeding. EC suspensions (10^6 cells/mL) were inoculated into the flow field and allowed to settle, attach, and spread out on the scaffold surface for 5 h before initiating flow.

EC viability assay

EC monolayers were assessed for viability using the Live/Dead Viability/Cytotoxicity Kit for mammalian cells (Invitrogen) according to kit instructions. Briefly, scaffolds were first rinsed in PBS, and then incubated for 30 min with 2 μM calcein AM and 2 μM ethidium homodimer-1. Images were captured as described next through both the GFP and DsRed filters to visualize live and dead cells, respectively.

EC staining

At the end of each experiment, scaffolds were rinsed in PBS, formalin fixed, and co-stained using rhodamine phalloidin (RP)/4′,6-diamidino-2-phenylindole, dihydrochloride (DAPI, 3 nM; Invitrogen). Imaging was conducted as described next in fluorescence microscopy.

EC retention analysis

EC co-stained with RP/DAPI as described earlier were separately imaged through each channel using multi-dimensional acquisition. Channel images obtained through the DAPI filter were exported for analysis using NIH ImageJ software. Imaging was conducted *in situ* within flow chambers to avoid distortion secondary to scaffold manipulation. Scaffolds were imaged in 10 predetermined locations per experimental condition and analyzed for cell density. DAPI images were analyzed using the ITCN Automatic Nuclei Counter plugin ver. 1.6 to quantify the number of cell nuclei in each image, which was divided by the image surface area to calculate cell density. Results are presented as mean ± standard deviation.

EC geometric parameter analyses

RP images obtained at 10× magnification were analyzed using the OrientationJ Measure plugin to determine actin fiber orientation with regard to the flow direction.[14] DAPI images obtained at 10× magnification were analyzed using the built-in particle analysis function of ImageJ to determine perimeter, area, and fit each nucleus with an ellipse to determine major axis orientation. The circularity (C) of each nucleus was calculated according to

$$C = \frac{4\pi A}{P^2} \tag{4}$$

where A is surface area and P is perimeter of each nucleus. The angle of the major axis was also determined with regard to the flow direction. Cells were individually analyzed within each 10× flow field to determine mean values for each geometric parameter ($n = 5$–7 images per condition).

Neutrophil adhesion to endothelialized HUV

GFP+ HL-60 cells were differentiated into neutrophil-like cells by exposure to 1.3% dimethy sulfoxide (Fisher Scientific) for 3 days, as previously described.[15] Endothelialized HUV scaffolds were activated for 4 h by adding 1 U recombinant human tumor necrosis factor-α (TNF-α; Thermo Scientific) to the media reservoir. Flow chambers were then removed from the incubator and placed on the stage of a Zeiss AxioImager M2 upright fluorescence microscope (Fig. 2A). Suspensions (10^6 cells/mL) of differentiated HL-60 cells (dHL-60) were then drawn through the flow chamber at a calculated wall SS of 1 dyne/cm^2 using a programmable syringe pump (Harvard Apparatus). Time lapse imaging of dHL-60 adhesion to endothelialized HUV was then performed over a 5 min period. Culture media without cells were allowed to flow through for an additional minute in order to remove non-adherent cells. Monolayers were fixed using 10% formalin and co-stained as described earlier.

For time lapse images, AxioVision software was used for frame-by-frame analysis in order to calculate firm adhesion duration and upstream/downstream rolling velocities for dHL-60 cells. Contrast enhancement was applied to each frame in order to determine a centroid and coordinate (x,y) for each cell. The distance traveled by each cell in consecutive frames was divided by the time elapsed in order to calculate mean upstream/downstream rolling velocities; only cells in steady motion were included (frames just before or immediately after firm adhesion in which the rolling velocity was changing were excluded in the analyses). Firm adhesion was determined to begin when the centroid coordinates did not change in consecutive frames; it was determined to end when the cell resumed rolling.

Scanning electron microscopy

HUV samples were fixed in 2.5% glutaraldehyde, washed in PBS, fixed in 1% osmium tetroxide solution, and progressively dehydrated in 25%, 50%, 75%. 85%, 95%, and 3×100% ethanol solutions. Samples were then critical point dried, sputter coated with gold/palladium, and imaged using a Hitachi S-4000 FE-SEM (10.0 kV).

Fluorescence microscopy

Imaging was conducted using a Zeiss AxioImager M2 upright fluorescence microscope coupled with an AxioCam HRm Rev. 3 digital camera operated by AxioVision software version 4.8.

Statistical analyses

One-way analysis of variance followed by *post-hoc* Tukey–Kramer HSD analyses (with the significance level set at 0.05) were conducted to compare EC density by experimental group or EC geometric parameters by time.

Results

Flow chamber design and assembly

A parallel-plate flow chamber was designed to perfuse fluid (culture media or peripheral blood) across an opaque substrate in an observable environment. Three design criteria were considered paramount: (1) that live imaging can be conducted under high magnification (40× or greater) for dynamic visualization of platelet adhesion, (2) that the device be capable of maintaining parabolic flow while accommodating scaffolds of various thicknesses, and (3) that the reagent volume required to fill the chamber be minimized to maximize use from limited volumes of peripherally drawn blood. A significant challenge was decreasing the distance between the top of the chamber and the substrate to allow the focal plane of the microscope objective to reach the scaffold surface. To accomplish this, a thin acrylic slide was bonded over two lanes forming the walls of the flow channel using clear epoxy resin (ITW Devcon 2 Ton Epoxy) to create a viewing window (Fig. 1A) with a total focal distance of 1.6 mm. With this design, a 40× Zeiss objective (LD Plan-Neofluar) with a maximum working distance of 2.9 mm was compatible for high-magnification imaging of cell adhesion within the flow chamber.

dHUV scaffolds of uniform thickness (750 μm), prepared as previously described,[7] were sliced open axially and affixed to acrylic base plates in a slightly tensed conformation using a compressible silicone gasket (Fig. 2A–C). The main body of the flow chamber was then screwed to the base plate, creating a sealed parallel plate flow channel with the bottom plate composed of the lumenal HUV surface (Fig. 2D, E). By minimizing the base width (*b*) and height (*h*) of the flow field (*b* 6.35×*h* 0.60 mm), the volume required to fill the flow channel was reduced to <300 μL, ~20% of the volume

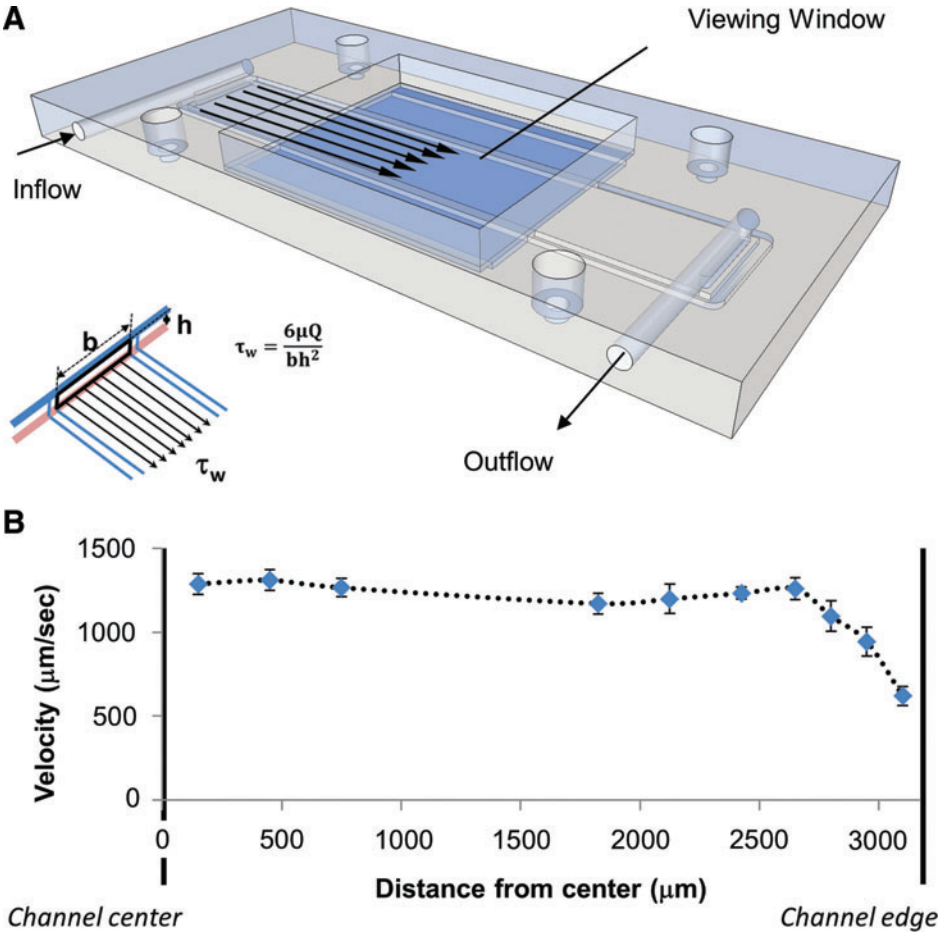

FIG. 1. Flow chamber design. The main body design of the flow chamber is shown in **(A)**. Culture media/cell suspensions are delivered through inflow/outflow ports. An acrylic viewing window was bonded to the center of the flow field to accommodate high-magnification imaging under flow. The flow field is composed of an acrylic chamber and substrate (not shown) in parallel plate geometry, which allows for simple shear stress (SS) calculations. The inset schematic shows how wall SS (τ_w) at the material's surface is calculated with regard to the flow field dimensions [see Eq. (1)]. **(B)** Velocity profile across the channel width. Mean flow velocity (presented as mean ± standard deviation [SD]) was calculated as a function of distance from the center of the channel. Velocity measurements were grouped as a function of distance from the center of the flow field base. Uniform flow velocity was observed across >90% of the channel width. Color images available online at www.liebertpub.com/tec

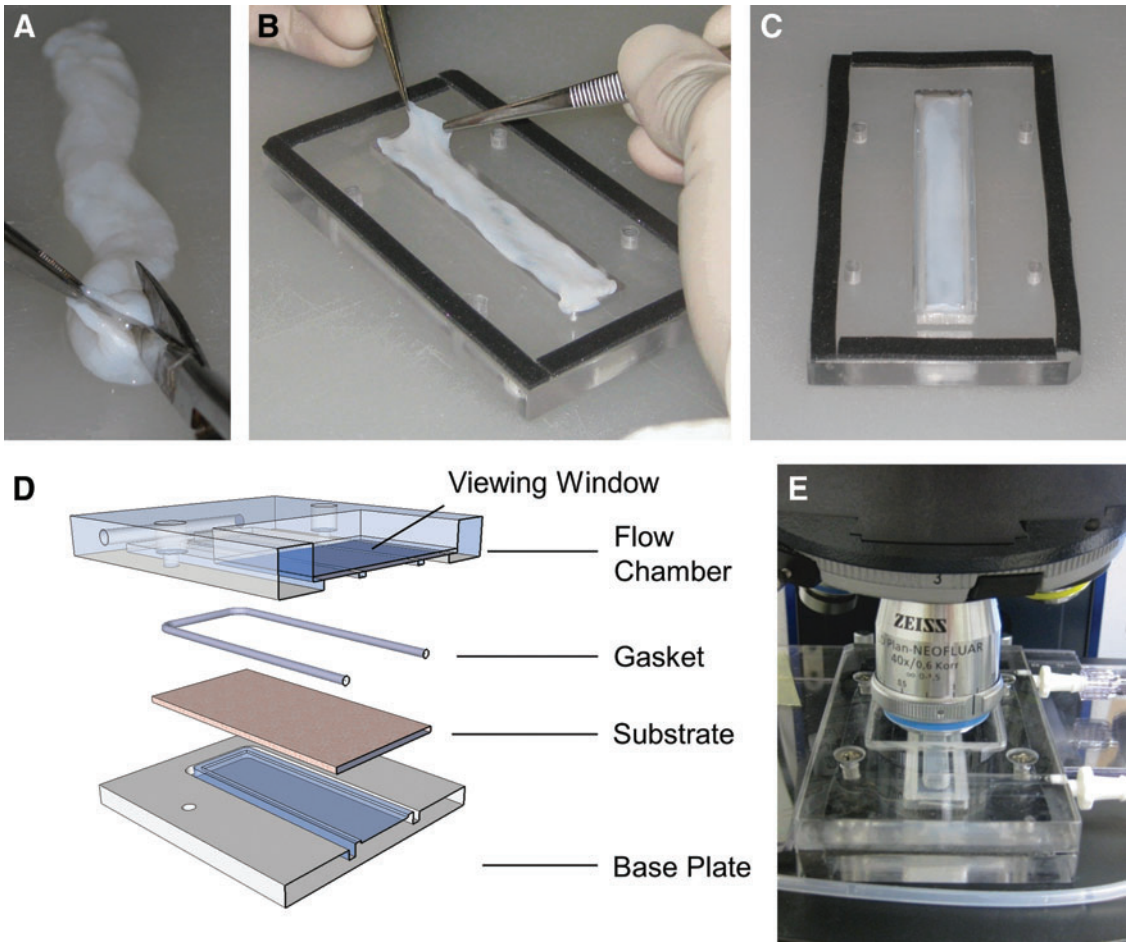

FIG. 2. Flow chamber assembly. Decellularized human umbilical vein (dHUV) scaffolds were cut open axially **(A)** and affixed to a base plate **(B)** using a compressible gasket **(C)**. The base plate was then tightly screwed to the flow chamber, creating a parallel plate flow profile across the HUV surface. A cross-sectional view of the various components is shown in **(D)**. Assembled flow chambers could then be placed on the stage of an upright epifluorescence microscope for high-magnification real-time imaging of adhesive interactions between fluorescently labeled cells and the scaffold's surface **(E)**. Color images available online at www.liebertpub.com/tec

of the native HUV vessel (average diameter 5–6 mm). No difference in mean flow velocity was observed across >90% of the channel width, indicating uniformity of flow (Fig. 1B).

Real-time observation of platelet adhesion

As an assessment of platelet adhesion, acridine orange-labeled whole blood was perfused across the acellular HUV and visualized at 40× magnification (Fig. 3A). Platelets were shown to progressively adhere to the surface, forming aggregates that elongated in the direction of flow. Coverage reached 3.7% of the total area over the 5 min perfusion period (Fig. 4). Measurement of aggregates' length parallel to the flow direction showed an elongation of all aggregates with an average length increase from 3.4 μm at 1 min to 11.6 μm at 5 min (Fig. 4B). The mean growth rate of platelet aggregates on the HUV surface was calculated as 68%/min (Fig. 4C).

Three-dimensional profiling of platelet aggregates

After 10 min of blood flow, numerous platelet aggregates had formed on the HUV basement membrane. Z-stack imaging was conducted to characterize the geometric distribution of platelets within aggregates in the *z*-direction (perpendicular to the surface). Twenty-five sections of two-dimensional images were collected at 2 μm stepped depths, and a composite image was created by combining the maximal intensity profiles of each *z*-stack image (Fig. 5A). Since the maximal intensity of each section corresponds to in-focus platelets, the light intensity of the composite 3D image correlates with the overall shape of the observed aggregate, with white representing the maximum height and black representing the minimum (Fig. 5B). Light intensity plots and 3D profiles of platelet aggregates were created using ImageJ plug-in Interactive 3D Surface Plot v2.33 (Fig. 5B–D).[16]

Light intensity profiles of seven aggregates were obtained and thresholded at a gray value of 100 to distinguish aggregates from the background (Fig. 6A). The skewness of the thresholded intensity profiles was then measured and showed these plots to be approximately symmetric with skewness values ranging from −0.06 to 0.2.[17] The normalized and averaged light intensity profile of the aggregates (Fig. 6B) showed a similar distribution of the data, with a

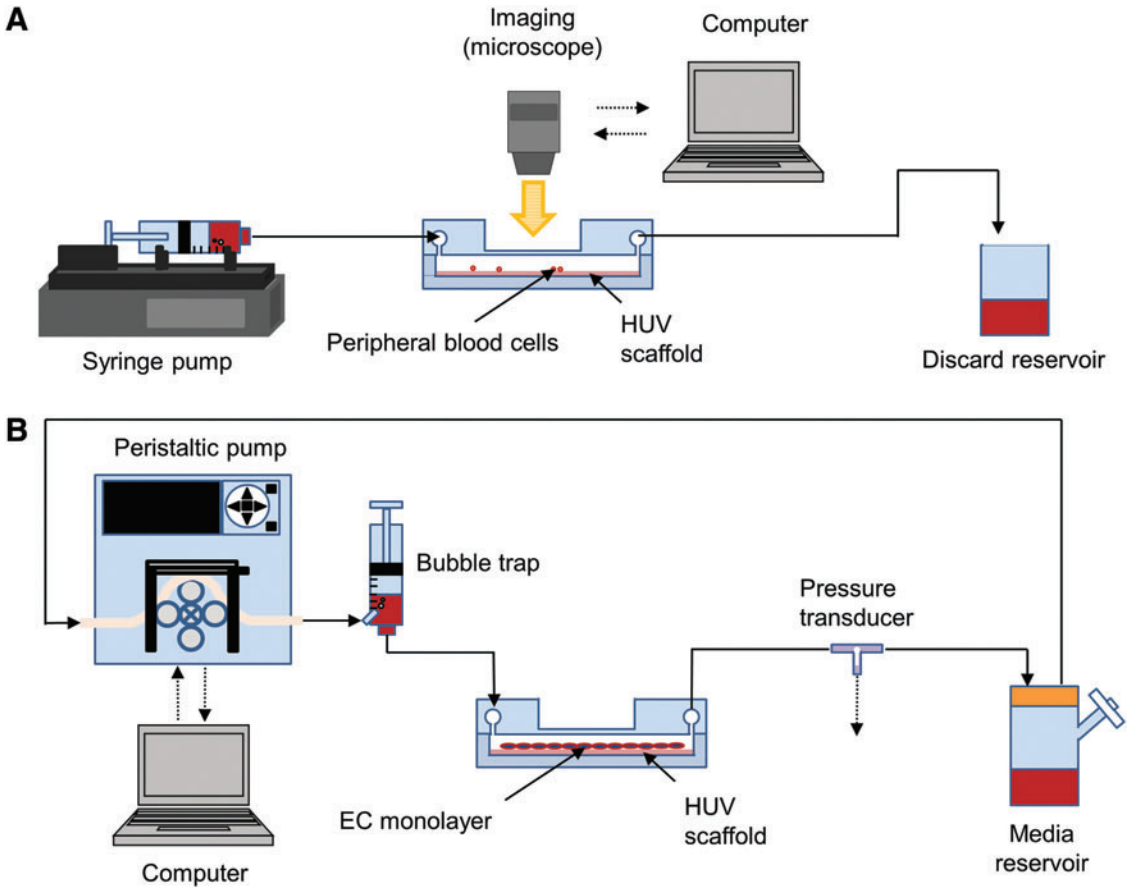

FIG. 3. Perfusion systems for imaging initial adhesion events or extended culture under flow. **(A)** Short-term imaging schematic. Syringe pumps were used to inject whole blood/cell suspensions through the flow chamber under defined shear conditions. A high-speed camera captured binding events of fluorescently labeled cells at high magnification through a long working distance microscope objective. **(B)** Long-term recirculating perfusion culture. Computer-controlled peristaltic pumps were used to modulate the flow across endothelialized HUV membranes. A bubble trap/pulse dampener was incorporated to abate endothelial cell (EC) denudation, while a pressure transducer was used to monitor pressure downstream of the flow chamber. Color images available online at www.liebertpub.com/tec

skewness value of 0.07 ± 0.05. Although the distribution was approximately symmetric, skewness data were slightly biased toward positive values, and analysis of the geometric profile of the plot in the flow direction showed a slightly more abrupt increase in light intensity upstream of the aggregate (linear increase with a slope of 3.2) with a more gradual decrease downstream (linear decrease with a slope of 2.5; Fig. 6B). In agreement with these measurements, the apex or maximal height of each platelet aggregate was typically located at the proximal (upstream) end.

Development of neo-endothelia on HUV scaffolds and adaptation to flow

Primary EC were seeded onto the lumenal surface of the HUV at an initial seeding density of 60,000 cells/cm^2, which correlated with a nearly confluent density for the same cells when cultured on polystyrene. After allowing the cells to adhere and spread out over the basement membrane for 5 h, endothelia were preconditioned over a 48 h period using one of the four strategies as indicated in Figure 7A. In Group 1, EC were exposed to low SS (0.3 dynes/cm^2, the minimum programmable flow rate for media exchange) for the entire period; this resulted in a high density of EC at the end of the preconditioning period (Fig. 7B). In Group 2, seeded EC were immediately exposed to high SS (6 dynes/cm^2, representing approximately half the desired mean SS value), which resulted in a significant decrease in cell density compared with group 1 (1264.92 ± 83.86 vs. 179.38 ± 38.57 cells/mm^2, $p = 0.000$). Based on the initial seeding density ($\sim$600 cells/mm^2), this suggested that immediate exposure to high SS caused the EC to strip off the lumenal surface.

To enable the EC to more gradually adapt to SS, Group 3 was designed in which the rotational speed of the pump was steadily ramped from 0.3 to 6 dynes/cm^2 over the 48 h period. This resulted in improvement of the cell density when compared with Group 2, but the cell density was significantly lower than in Group 1 (1264.92 ± 83.86 vs. 640.17 ± 110.84 cells/mm^2, $p = 0.000$). To allow the EC additional time to mature on the HUV surface, Group 4 was designed in which the cells were cultured under low SS (0.3 dynes/cm^2) for the first 24 h, and then exposed to ramped flow (0.3–6 dynes/cm^2) over the second 24 h. This strategy resulted in a similar cell density as Group 1, with no statistically significant difference between these two groups (1264.92 ± 83.86 vs. 1236.00 ± 169.30 cells/mm^2, $p = 0.969$).

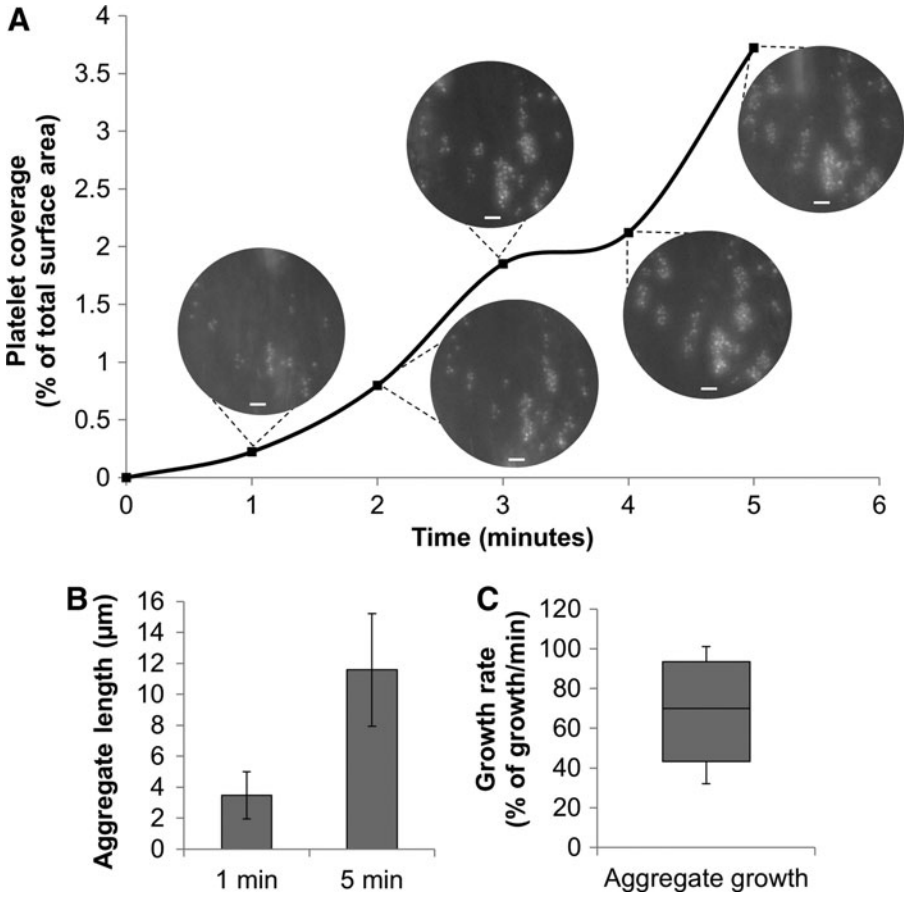

FIG. 4. Real-time observation of platelet adhesion to acellular HUV. Whole blood was perfused across the surface of dHUV at a SS of 2 dynes/cm^2. Platelet adhesion and aggregation was imaged via epifluorescence microscopy and quantified over a 5 min period **(A)**. Scale bars: 10 μm. Elongation of the aggregates formed was further analyzed by observing aggregate length at 1 and 5 min **(B)**, as well as growth rate of the aggregates **(C)**. Box plot shows the range, first–third quartiles (shaded region), and median (dark line) for aggregate growth.

Further experiments were conducted using the shear preconditioning strategy described in Group 4.

Shear conditioning of neo-endothelia

We next used the device to assess the potential of the dHUV to support an EC monolayer under physiological SS conditions for experimentally relevant time periods. Endothelia were conditioned to SS by ramping the flow rate as indicated in Figure 8A. Cytoskeletal F-actin filaments aligned parallel to the flow direction, and a significant decrease in the average filament angle relative to the shear direction was observed after flow ramping was initiated (Fig. 8C). This correlated with nucleus alignment in the flow

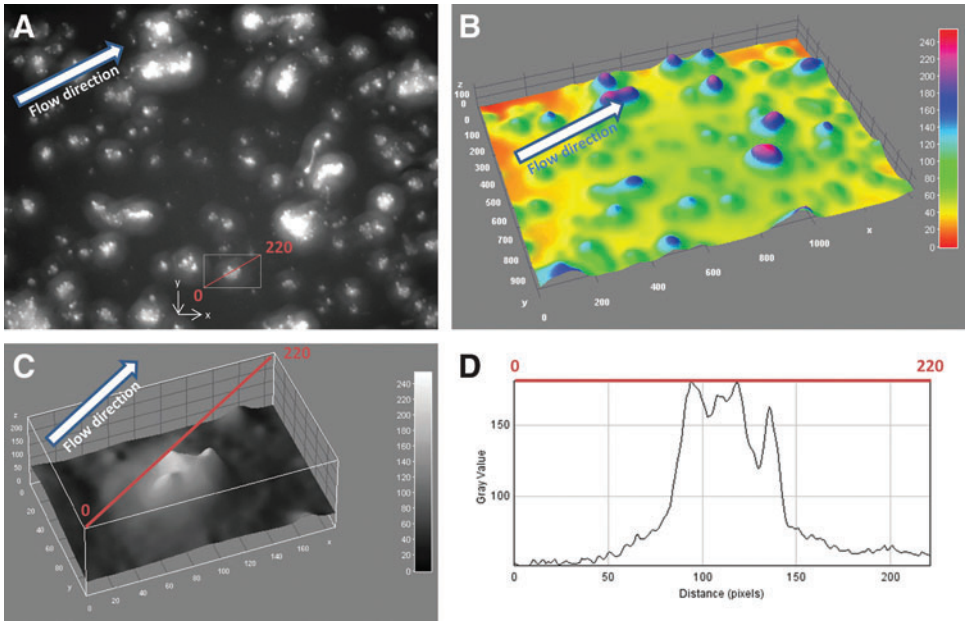

FIG. 5. Flow-induced platelet aggregate geometries. Whole blood was perfused over the surface of dHUV at a SS of 2 dynes/cm^2. After 10 min, 25 *z*-stack images were taken at 2 μm steps. A composite image of the maximum intensity areas from all 25 images is presented in **(A)**, and a three-dimensional (3D) light intensity profile of this composite is shown in **(B)**. The platelet aggregate framed in **(A)** was further analyzed along the 220 pixel cross-sectional red line, and both 3D and two-dimensional light intensity profiles of this aggregate are presented in **(C)** and **(D)**, respectively. Color images available online at www.liebertpub.com/tec

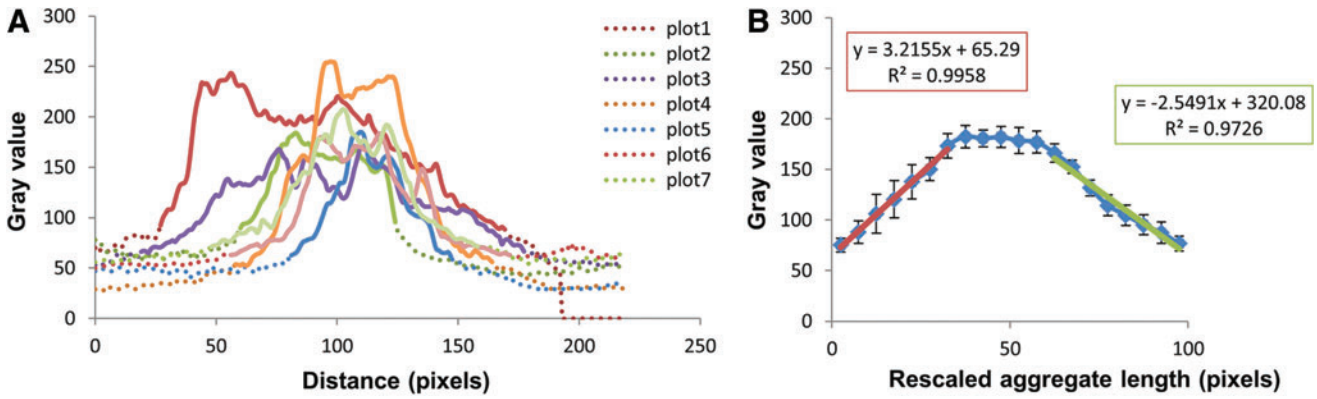

FIG. 6. Light intensity profile of platelet aggregates. Light intensity profiles of seven platelet aggregates from the composite image presented in Figure 5A were measured **(A)**. A threshold was applied to distinguish each platelet aggregate from background (HUV surface), and the length of the thresholded plots (represented as a solid line in Fig. 6A) was rescaled out of 100 pixels. The gray value of all plots was then averaged across five pixels increments. The average profile of the seven platelet aggregates after normalization is shown in **(B)**. The red and green lines represent the upstream and downstream slopes, respectively, of the composite profile. Color images available online at www.liebertpub.com/tec

direction (Fig. 8D). Progressive nuclear elongation was observed after physiological levels of SS had been applied (Fig. 8E). Two days after seeding, a confluent EC monolayer was developed that was able to withstand SS commonly found in small diameter arteries, confirmed by an additional day of perfusion culture. Confluent neo-endothelia were maintained under pulsatile perfusion (mean ± amplitude 12 ± 12 dynes/cm^2 at 80 pulses/min) for approximately 7 days after seeding (Fig. 8B).

Morphological comparison of endothelia cultured under static culture or flow conditions

Neo-endothelia cultured on the opaque lumenal surface of dHUV (as described above) were subjected to either pulsatile SS (12 ± 12 dynes/cm^2 at 80 pulses/min) or static culture conditions for 24 h. Scanning electron microscopy (SEM) taken from an oblique (45°) angle relative to the HUV surface show EC cultured under flow to have a significantly more

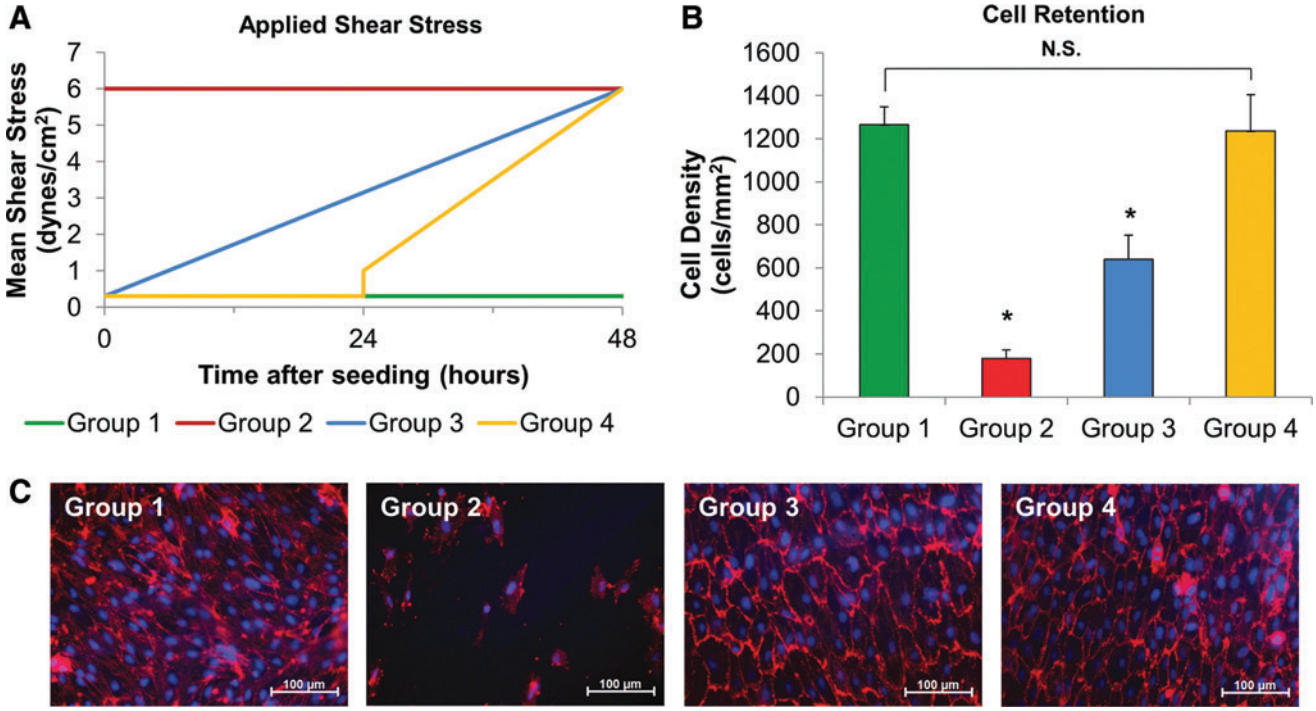

FIG. 7. Shear preconditioning strategies for EC-seeded HUV scaffolds. dHUV grafts were cut open axially and secured in the flow chamber as described earlier. Primary EC were seeded onto the lumenal surface, and 5 h later, they were adapted to flow using various shear preconditioning strategies **(A)**. After 48 h, the average cell density was quantified from each group **(B)**. Results are presented as mean ± SD (n = 5–7 10× images per group). Asterisks indicate a significant difference relative to Group 1. Representative images of the lumenal surface from each group are shown in **(C)**. Scale bar: 100 µm. N.S. indicates no significant difference in mean cell density. Color images available online at www.liebertpub.com/tec

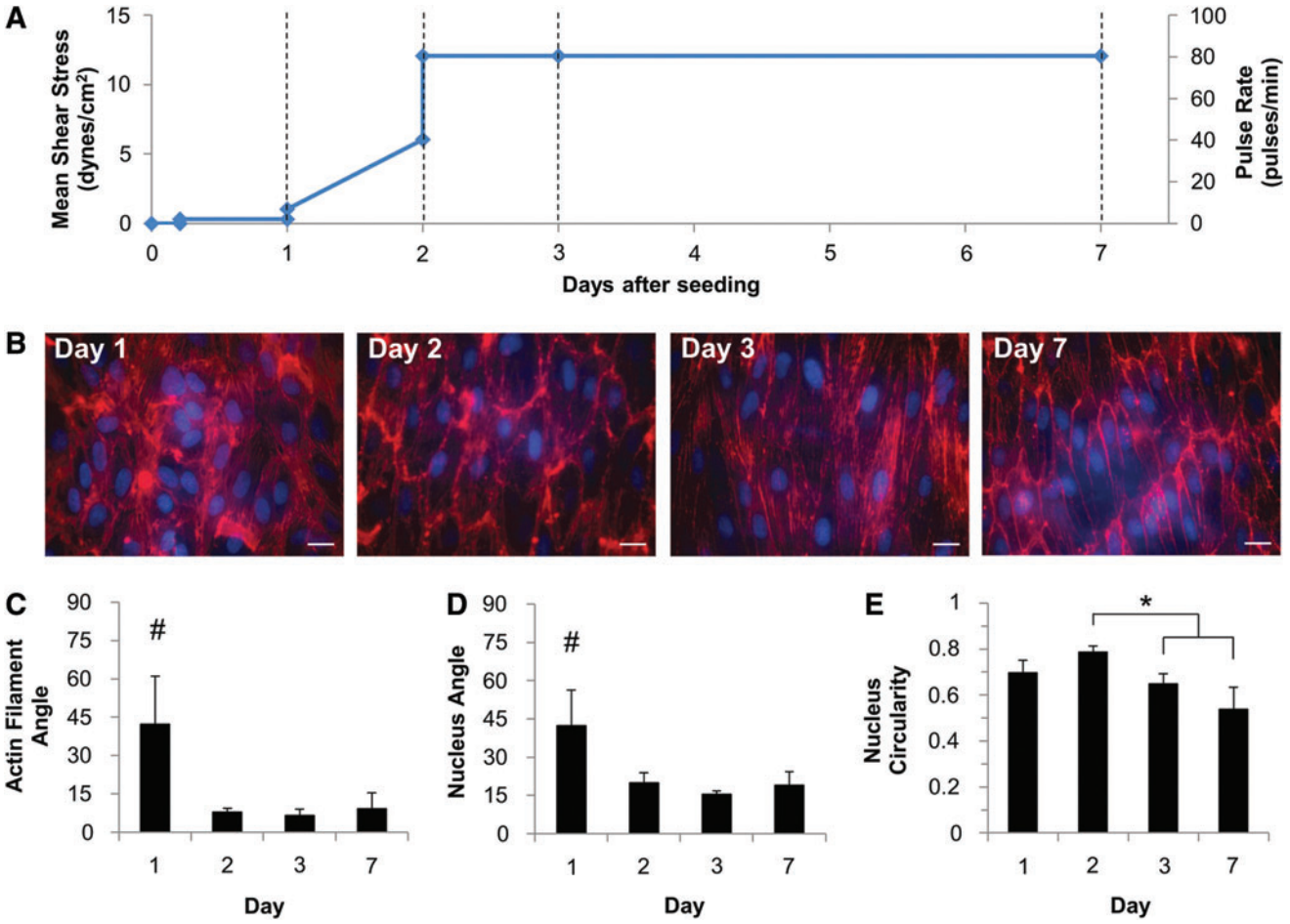

FIG. 8. Maturation of endothelialized HUV scaffolds. dHUV scaffolds were affixed to flow chambers as described earlier. EC were seeded onto the lumenal HUV surface at a high concentration and gradually adapted to flow using computer-controlled peristaltic pumps. The calculated mean wall SS along the lumenal HUV surface over the culture period is shown in **(A)**. At various time points (indicated by the dashed lines), monolayers were fixed and co-stained with rhodamine phalloidin (RP)/4′,6-diamidino-2-phenylindole, dihydrochloride (DAPI) to visualize F-actin/cell nuclei, respectively. Representative images of EC morphology at 1, 2, 3, and 7 days after seeding are shown in **(B)**. Actin filament angle **(C)** was quantified using the OrientationJ plugin of ImageJ, and nucleus major axis angle **(D)** and circularity **(E)** were quantified using the built-in functions of ImageJ. Results are presented as mean ± SD values for each parameter ($n = 5$–7 10× images per time point). Asterisk indicates significant differences in mean as specified, and "#" indicates significant differences in mean relative to all other time points. Scale bars: 20 μm. Color images available online at www.liebertpub.com/tec

flattened morphology, with less variation in height than static-cultured cells (Fig. 9A, B). This finding correlated with cellular elongation in the flow direction (Fig. 9E, F), which accounts for the reduced topographical variation between cell–cell junctions that is visible in SEM images. Calcein/ethidium co-staining confirmed a high proportion of viable cells on endothelial monolayers cultured on the HUV basement membrane, and exposure to arterial SS levels had no deleterious effect on cellular viability (Fig. 9C, D).

Real-time observation of neutrophil rolling on neo-endothelia

For functional assessment of neo-endothelia, we designed a system to image rolling adhesion and arrest of human leukocytes under flow. After 3 days of flow conditioning, EC monolayers were activated with recombinant human TNF-α to stimulate cell adhesion molecule expression. Time lapse imaging conducted at 10× magnification (for observing a larger surface area) captured rolling adhesion and arrest of GFP-expressing neutrophil-like dHL-60 cells over a 5 min period (Fig. 10A). Quantification of adherent cells in each frame showed a roughly linear increase that reached a plateau after 4 min. RP/DAPI co-staining confirmed the presence of a confluent EC monolayer beneath adherent dHL-60, which predominantly localized at cell–cell junctions (Fig. 10B). Firm adhesion lasted an average of 29.1 ± 15.9 s per event, and dHL-60 rolling velocity was generally higher after firm adhesion than earlier (Fig. 10C, D).

Discussion

Several techniques have been developed for visualizing the dynamic events associated with platelet aggregation/leukocyte adhesion on vascular biomaterials *in vitro*, where biochemical factors, mechanical stimuli, and interactions

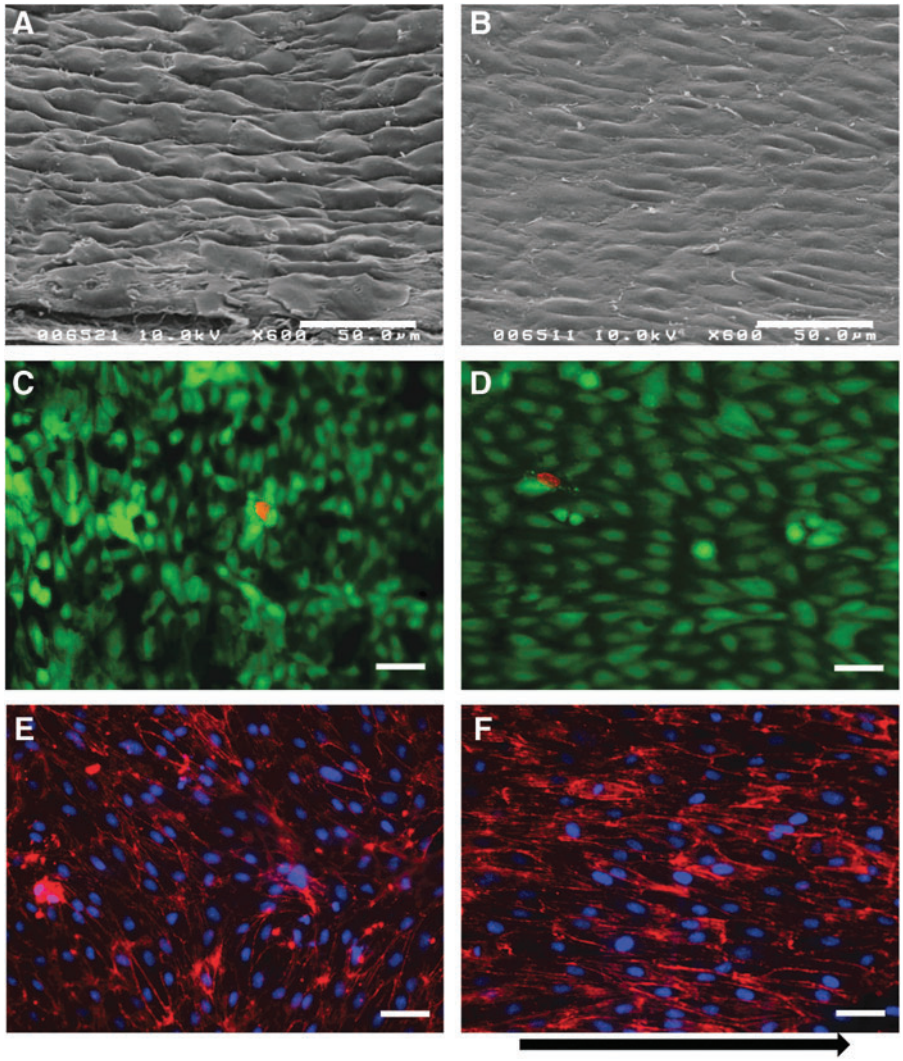

FIG. 9. Morphological comparison of endothelia cultured under static culture or flow conditions. Processed HUV scaffolds were fit in custom-designed flow chambers as previously described. Primary EC suspensions were injected into the flow field and either cultured under static conditions **(A**, **C**, **E)** or adapted to flow **(B**, **D**, **F)** over a 72 h period. Scanning electron micrographs of endothelialized HUV scaffolds at oblique angle show the more flattened morphology under flow **(B)** than under static culture **(A)**. Calcein/ethidium live/dead staining reveals high cellular viability in static culture **(C)** or under SS **(D)**. F-actin/DAPI staining shows cytoskeletal F-actin (red)/cell nuclei (blue) **(E**, **F)**. Arrow (below panel F) shows the flow direction in **(B)**, **(D)**, and **(F)**. Scale bars: 50 μm. Color images available online at www.liebertpub.com/tec

with isolated cell populations can be precisely controlled.[18] Systems used for imaging isolated blood vessels/vascular grafts *ex vivo* are particularly suited for observing agonist-induced contraction/dilation and other whole-vessel responses,[19] but have limitations for observing intimal phenomena due to an increase in light scattering coupled with the loss of resolution associated with thicker, opaque vessels. Alternatively, harvested vessels can be opened longitudinally to directly image cells adhered to the lumenal surface, but this does not permit real-time imaging of cell accumulation under flow.[20]

Parallel-plate flow chambers have been used for decades to study behavior of particular cell populations under controlled flow conditions.[8] These devices have several advantages compared with tubular *ex vivo*-derived or engineered vessels: lower reagent requirements, more uniform SS fields, and enhanced imaging clarity compared with intravital microscopy. To overcome the limitations associated with imaging through opaque tissue scaffolds, we designed a novel flow chamber that holds a compliant vascular biomaterial in a stable conformation such that SS across the wall can be precisely controlled. The graft is cut open longitudinally and secured between two plates, allowing the intimal surface to be directly imaged while fluorescently labeled whole blood/select cell suspensions are perfused across. This permits live imaging using conventional epifluorescence microscopy techniques. Using this design, we characterized the early binding properties of the HUV scaffold under simulated blood flow.

The HUV has several ideal properties that allow it to serve as a vascular allograft: The vessel has an adequate length (50–60 cm), is free of bifurcations, and can readily be obtained hospital delivery wards.[21] The HUV has been used in vascular reconstruction surgeries for more than 30 years,[22] and, more recently, it has been developed as an *ex vivo*-derived vascular scaffold for tissue engineering applications.[13,23] Due to its clinical relevance, the HUV served as an excellent model to assess a vascular biomaterial for both modeling platelet/neutrophil adhesion and endothelialization under flow.

Decellularization of the HUV using SDS has previously been shown to leave behind an intact basement membrane that can be repopulated with EC.[24] Spontaneous EC ingrowth or "in situ endothelialization" rarely occurs in humans on prosthetic grafts.[25] Therefore, a goal for tissue

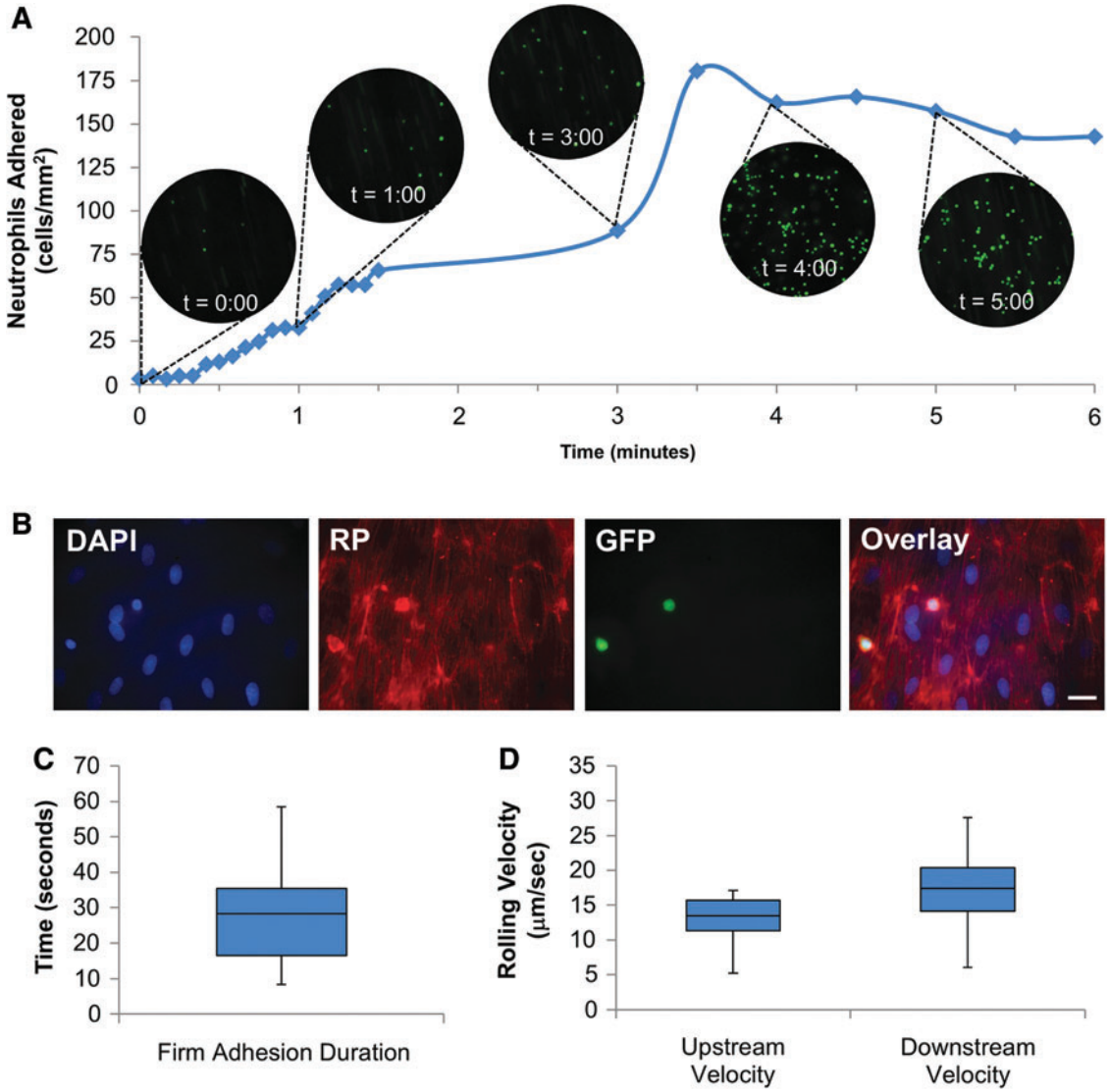

FIG. 10. Time-lapse capture of neutrophil adhesion to endothelialized HUV scaffolds. Endothelia adapted to flow were activated with 1 U tumor necrosis factor-α. A bolus of dHL-60 was then flowed across the lumenal HUV surface at a calculated SS of 1 dyne/cm^2. Time-lapse imaging captured adhesion of green fluorescent protein (GFP)+ dHL-60 cells to the activated endothelia over 5 min **(A)**. Shown are images at various time points throughout the experiment. After dHL-60 cells were allowed to flow across the surface, non-adherent cells were washed away, and scaffolds were fixed and co-stained with RP/DAPI. Multi-dimensional images show a confluent endothelial monolayer with adherent GFP+ dHL-60 cells **(B)**. DAPI: cell nuclei; RP: F-actin; GFP: GFP+ dHL-60 cells. Scale bar: 25 μm. Additional box plots **(C)** demonstrate the firm adhesion duration and rolling velocities **(D)** measured before (upstream) or after (downstream) firm adhesion occurred. Box plots show the range, first–third quartiles (shaded region), and median (dark line) for each parameter. Color images available online at www.liebertpub.com/tec

engineered grafts is to produce a lumenal surface that is both resistant to platelet aggregation and favorable for EC regrowth. The flow chamber allows a temporal observation of EC proliferation and morphological adaptation to SS *in situ*. To avoid stripping EC off the HUV surface by the sudden onset of flow, cells were shear conditioned by progressively increasing flow rates until approximately physiological levels of arterial wall SS were reached. Adaptation of EC on other vascular biomaterials to physiological SS levels could similarly be optimized using this device in preparation for implantation of preseeded constructs in the aggressive arterial circulation.

Platelet adhesion/aggregation onto vascular grafts is directly related to their propensity to adsorb plasma proteins, which is dependent on surface hydrophilicity, electric charge, and chain mobility.[26] It is the combination of these factors that determines the thrombogenicity of a material and makes its *in vivo* performance difficult to predict. Previously, it was shown that the dHUV scaffold is resistant to platelet adhesion, though comparatively favorable for attachment of EC under static conditions.[24] However, platelet

adhesion to proteins is highly dependent on local hemodynamic shear trends, and graft thrombogenicity is more accurately assessed under dynamic conditions.[27] In the present study, we observed a temporally increasing trend of platelet adhesion and aggregate formation to the processed vascular scaffold, leading to 3.7% coverage of the total surface area over a 5 min perfusion period. This shows the denuded HUV scaffold to be more prone to platelet adhesion under the shear conditions applied than was previously thought under static incubation (<1% coverage).[24] Real-time light intensity profiles showed the aggregates to have a steep height increase upstream with a more gradual decrease downstream, similar to observations made in collagen type I coated glass slides.[28] As such, this system offers a rapid method using a modified parallel plate flow chamber to assess these materials in a high throughput approach.

In summary, we have designed and characterized a novel flow chamber using *ex vivo*-derived vascular tissue for *in vitro* modeling of cell adhesion events in an environment that is more reminiscent of the natural vasculature. We have demonstrated functional uses of this device for investigating cell adhesion events during normal vascular homeostasis or in response to injury. The design presented can be used for preimplantation screening of a wide range of other biomaterials to assess blood cell interactions.

Acknowledgments

The authors would like to acknowledge the National Institutes of Health for funding R01-HL088207 and R01-HL088207-03S1. They thank Alan Miles for providing flow chamber machining consultation. The authors would also like to thank the Electron Microscopy and Bio-imaging Laboratory at UF for technical assistance, Christopher Cogle and the UF Clinical and Translational Science Institute for their assistance with blood draws. They also thank Dr. Cogle for contributing the GFP+ HL-60 cells for this study.

Disclosure Statement

The authors have no conflicts of interest to declare.

References

1. Mehta, D., Izzat, M.B., Bryan, A.J., and Angelini, G.D. Towards the prevention of vein graft failure. Int J Cardiol **62 Suppl 1,** S55, 1997.
2. Kannan, R.Y., Salacinski, H.J., Butler, P.E., Hamilton, G., and Seifalian, A.M., Current status of prosthetic bypass grafts: a review. J Biomed Mater Res B Appl Biomater **74,** 570, 2005.
3. Kapadia, M.R., Popowich, D.A., and Kibbe, M.R. Modified prosthetic vascular conduits. Circulation **117,** 1873, 2008.
4. Sarkar, S., Sales, K.M., Hamilton, G., and Seifalian, A.M. Addressing thrombogenicity in vascular graft construction. J Biomed Mater Res B Appl Biomater **82,** 100, 2007.
5. L'Heureux, N., Dusserre, N., Konig, G., Victor, B., Keire, P., Wight, T.N., *et al.* Human tissue-engineered blood vessels for adult arterial revascularization. Nat Med **12,** 361, 2006.
6. Yazdani, S.K., Tillman, B.W., Berry, J.L., Soker, S., and Geary, R.L. The fate of an endothelium layer after preconditioning. J Vasc Surg **51,** 174, 2010.
7. Hanson, S.R., Kotze, H.F., Savage, B., and Harker, L.A. Platelet interactions with Dacron vascular grafts. A model of acute thrombosis in baboons. Arteriosclerosis **5,** 595, 1985.
8. Frangos, J.A., Eskin, S.G., McIntire, L.V., and Ives, C.L. Flow effects on prostacyclin production by cultured human endothelial cells. Science **227,** 1477, 1985.
9. Bacabac, R.G., Smit, T.H., Cowin, S.C., Van Loon, J.J., Nieuwstadt, F.T., and Heethaar, R., *et al.* Dynamic shear stress in parallel-plate flow chambers. J Biomech **38,** 159, 2005.
10. Reinhart-King, C.A., Fujiwara, K., and Berk, B.C. Physiologic stress-mediated signaling in the endothelium. Methods Enzymol **443,** 25, 2008.
11. Schmidtke, D.W., and Diamond, S.L. Direct observation of membrane tethers formed during neutrophil attachment to platelets or P-selectin under physiological flow. J Cell Biol **149,** 719, 2000.
12. Jaffe, E.A., Nachman, R.L., Becker, C.G., and Minick, C.R. Culture of human endothelial cells derived from umbilical veins. Identification by morphologic and immunologic criteria. J Clin Invest **52,** 2745, 1973.
13. Daniel, J., Abe, K., and McFetridge, P.S. Development of the human umbilical vein scaffold for cardiovascular tissue engineering applications. ASAIO J **51,** 252, 2005.
14. Rezakhaniha, R., Agianniotis, A., Schrauwen, J.T., Griffa, A., Sage, D., Bouten, C.V., *et al.* Experimental investigation of collagen waviness and orientation in the arterial adventitia using confocal laser scanning microscopy. Biomech Model Mechanobiol **11,** 461, 2012.
15. Mollinedo, F., López-Pérez, R., and Gajate, C. Differential gene expression patterns coupled to commitment and acquisition of phenotypic hallmarks during neutrophil differentiation of human leukaemia HL-60 cells. Gene **419,** 16, 2008.
16. Barthel, K.U. Interactive 3D Surface Plot v2.33 plug-in for ImageJ. Internationale Medieninformatik, 2011. http://rsb.nih.gov/ij/plugins/surface-plot-3d.html
17. Bulger, M.G. Principles of Statistics, 2nd edition. Maneola, NY: Dover Publications, Inc., 1979.
18. Michell, D.L., Andrews, K.L., Woollard, K.J., and Chin-Dusting, J.P. Imaging leukocyte adhesion to the vascular endothelium at high intraluminal pressure. J Vis Exp pii: 3221, 2011.
19. Butler, P.J., Weinbaum, S., Chien, S., and Lemons, D.E. Endothelium-dependent, shear-induced vasodilation is rate-sensitive. Microcirculation **7,** 53, 2000.
20. Bolick, D.T., Srinivasan, S., Kim, K.W., Hatley, M.E., Clemens, J.J., Whetzel, A., *et al.* Sphingosine-1-phosphate prevents tumor necrosis factor-{alpha}-mediated monocyte adhesion to aortic endothelium in mice. Arterioscler Thromb Vasc Biol **25,** 976, 2005.
21. Ente, G., and Penzer, P.H. The umbilical cord: normal parameters. J R Soc Health **111,** 138, 1991.
22. Dardik, H. A 30-year odyssey with the umbilical vein graft. J Am Coll Surg **203,** 582, 2006.
23. Tosun, Z., Villegas-Montoya, C., and McFetridge, P.S. The influence of early-phase remodeling events on the biomechanical properties of engineered vascular tissues. J Vasc Surg **54,** 1451, 2011.
24. Uzarski, J.S., Van De Walle, A.B., and McFetridge, P.S. Preimplantation processing of *ex vivo*-derived vascular biomaterials: effects on peripheral cell adhesion. J Biomed Mater Res A **101,** 123, 2012.

25. Zilla, P., Bezuidenhout, D., and Human, P. Prosthetic vascular grafts: wrong models, wrong questions and no healing. Biomaterials **28,** 5009, 2007.
26. Hu, W.J., Eaton, J.W., Ugarova, T.P., and Tang, L. Molecular basis of biomaterial-mediated foreign body reactions. Blood **98,** 1231, 2001.
27. Schneider, S.W., Nuschele, S., Wixforth, A., Gorzelanny, C., Alexander-Katz, A., and Netz, R.R., *et al.* Shear-induced unfolding triggers adhesion of von Willebrand factor fibers. Proc Natl Acad Sci U S A **104,** 7899, 2007.
28. Tolouei, E., Butler, C.J., Fouras, A., Ryan, K., Sheard, G.J., and Carberry, J. Effect of hemodynamic forces on platelet aggregation geometry. Ann Biomed Eng **39,** 1403, 2011.

Address correspondence to:
Peter S. McFetridge, PhD
J. Crayton Pruitt Family Department of Biomedical Engineering
University of Florida
Biomedical Sciences Building, JG-56
1275 Center Drive
P.O. Box 116131
Gainesville, FL 32611-6131

E-mail: pmcfetridge@bme.ufl.edu

Received: December 28, 2012
Accepted: May 15, 2013
Online Publication Date: August 23, 2013